

Electronic Supplementary Information

Lenvatinib and Cu_{2-x}S nanocrystals co-encapsulated in poly(D,L-lactide-co-glycolide) for synergistic chemophotothermal therapy against advanced hepatocellular carcinoma

Qi Xu ^{a,1}, Qiuting Li ^{c,1}, Zhe Yang ^d, Piao Huang ^a, Han Hu ^a, Zhimin Mo ^a, Zizhen Qin ^a, Zushun Xu ^a, Tianyou Chen ^{a,*}, Shengli Yang ^{b,**}

^a Ministry of Education Key Laboratory for the Green Preparation and Application of Functional Materials, Hubei Key Laboratory of Polymer Materials, Hubei Collaborative Innovation Center for Advanced Organic Chemical Materials, School of Materials Science and Engineering, Hubei University, Wuhan 430062, China

^b Cancer Center, Union Hospital, Tongji Medical College of Huazhong University of Science and Technology, Wuhan, Hubei, 430022, China

^c Department of Oncology, Liyuan Hospital, Tongji Medical College, Huazhong University of Science and Technology, Wuhan 430077, China

^d Department of Chemistry, City University of Hong Kong, Hong Kong, China

¹ Qi Xu and Qiuting Li contributed equally to this work.

*Email: tianyou.chen@hubu.edu.cn

**Email: yangshengli2014@yahoo.com

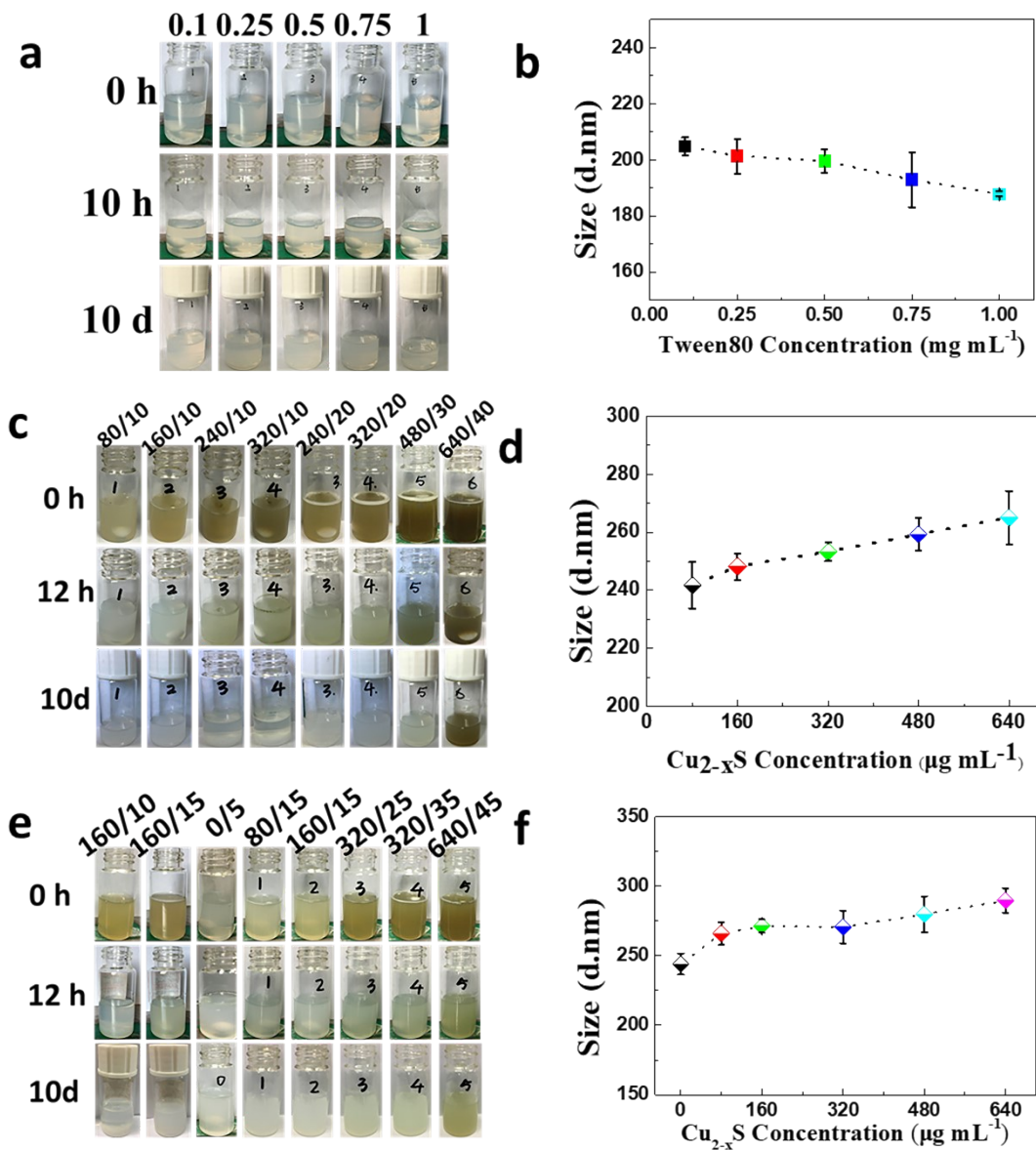


Fig. S1 (a)(c)(e) Digital photographs of PLGA NPs/Cu_{2-x}S@PLGA NPs/Cu_{2-x}S-LT@PLGA NPs with different nanoprecipitation conditions; (b)(d)(f) and their DLS analysis.

Calculation of the photothermal conversion efficiency

The calculation process is as follows¹:

$$\text{The total energy balance equation in the system: } \sum_i m_i C_{p,i} \frac{dT}{dt} = Q_{\text{NPs}} = Q_s - Q_{\text{loss}} \quad (1);$$

Where m_i and C_p are mass and heat capacity respectively. The suffix 'i' refers to solvent (water) or dispersion (nanoparticle). T is the temperature of the solution. Q_{NPs} are the light and heat energy absorbed by $\text{Cu}_{2-x}\text{S} @\text{PLGA}$ NPs per second:

$$Q_{\text{NPs}} = I(1-10^{-A_\lambda})\eta \quad (2);$$

Where I is the laser power, A_λ is the absorbance of $\text{Cu}_{2-x}\text{S} @\text{PLGA}$ NPs in a 1064 nm aqueous solution, and η is the photothermal conversion efficiency of $\text{Cu}_{2-x}\text{S} @\text{PLGA}$ NPs, that is, the ratio of absorbed light energy conversion to heat energy.

$$Q_{\text{LOSS}} \text{ refers to the heat energy lost to the surrounding environment: } Q_{\text{loss}} = hA\Delta T \quad (3);$$

Among them, h is the heat transfer coefficient, A is the surface area of the container, and ΔT is the temperature change, that is, $T - T_{\text{surr}}$ (T and T_{surr} are the solution temperature and the ambient temperature, respectively).

Q_s is the heat generated by the laser light absorbed by the solvent every second. In the case of heating pure water, the heat input is equal to the heat output at the highest steady-state temperature, so the equation is: $Q_s = Q_{\text{loss}} = hA\Delta T_{\text{max,H}_2\text{O}}$ (4);

$\Delta T_{\text{max,H}_2\text{O}}$ is the temperature change of water at the highest steady-state temperature. In the $\text{Cu}_{2-x}\text{S} @\text{PLGA}$ NPs dispersion experiment, the heat input is the heat generated by nanoparticles (Q_{NPs}) and the heat generated by water (Q_s), which is equal to the heat output at the highest steady-state temperature, so the equation can be: $Q_{\text{NPs}} + Q_s = Q_{\text{loss}} = hA\Delta T_{\text{max,min}}$ (5);

$\Delta T_{\text{max,min}}$ is the temperature change of $\text{Cu}_{2-x}\text{S} @\text{PLGA}$ NPs dispersion at the highest steady-state temperature.

According to formulas (2), (4) and (5), the light-to-heat conversion efficiency (η) can be expressed as:

$$\eta = \frac{hA\Delta T_{max,min} - hA\Delta T_{max,H2O}}{I(1 - 10^{-A}\lambda)} = \frac{hA(\Delta T_{max,min} - \Delta T_{max,H2O})}{I(1 - 10^{-A}\lambda)} \quad (6);$$

In this equation, only hA is unknown. In order to obtain hA, we introduce θ , which is

$$\text{defined as the ratio of } \Delta T \text{ to the maximum } \Delta T_{max}: \theta = \frac{\Delta T}{\Delta T_{max}} \quad (7);$$

$$\text{Bring (7) into (1) to get: } \frac{d\theta}{dt} = \frac{hA}{\sum_i m_i C_{p,i}} \left[\frac{Q_{NPs} + Q_s}{hA\Delta T_{max}} - \theta \right] \quad (8);$$

When the laser is off, $Q_{NPs} + Q_s = 0$, then (8) is:

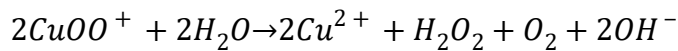
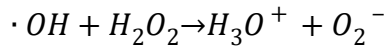
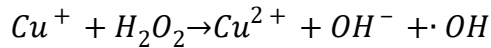
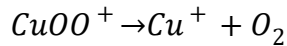
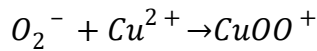
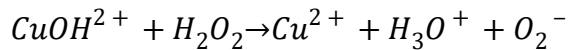
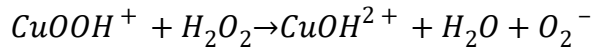
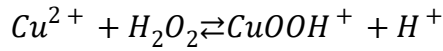
$$dt = - \frac{\sum_i m_i C_{p,i}}{hA} \frac{d\theta}{\theta} \quad (9); \quad (9) \text{ Can be transformed into: } t = - \frac{\sum_i m_i C_{p,i}}{hA} \ln\theta \quad (10);$$

$\frac{\sum_i m_i C_{p,i}}{hA}$ can be obtained from the $t - \ln\theta$ curve. Compared with the solvent (water, 800 mg), the mass of the nanoparticles (0.512 mg) is too small. Generally speaking, the specific heat of water is much higher than other materials, so m_{NPs} and $C_{p,NPs}$ can be ignored.

In this experiment, as shown in the figure (Fig.3 k,l) $t - \ln\theta$ fitting curvey = 155.38234x - 77.18748, $m_{H_2O} = 0.8$ g, $C_{p,H_2O} = 4.2$ J (g °C)⁻¹, $hA = 0.02162$, $A_\lambda (1064) = 1.3177$, $\Delta T_{max,min} = 31.3$ °C, $\Delta T_{H_2O,min} = 4$ °C, $I = 0.84$ W, Energy Density = 0.84 W/0.55 cm² = 1.5 W cm⁻², then $\eta = 31.07\%$.

Mechanism of catalytic action of Cu(II) on the decomposition of H₂O₂

Cu⁺ can react with H₂O₂ to generate ·OH (k=4.6×10² M⁻¹s⁻¹) and Cu²⁺; Cu²⁺ can react with H₂O₂ to generate HO₂· and Cu⁺ (k=1×10⁴ M⁻¹s⁻¹) via a Fenton-like reaction ². In addition, Cu²⁺ can catalyze the decomposition of H₂O₂ to generate oxygen. It is more inclined to produce ·OH by Cu⁺, and the rate of Cu²⁺ catalyzed reaction is lower. As a catalyst for H₂O₂ decomposition, Cu²⁺ has high catalytic efficiency. The kinetic data so far available on the Cu²⁺-catalyzed decomposition of hydrogen peroxide indicate that this reaction follows a rather complex mechanism. Although more experimental information is required to establish the reaction mechanism, a plausible sequence of elementary steps for the reaction might be the following ³:



Glutathione determination

Intracellular GSH was measured as described by instruction of the GSH and GSSG Assay Kit. First, MHCC97H cells were plated in cell culture dish and incubated overnight. Then cells were incubated with 100 μ L PBS, 4mM free Lenvatinib, 500 mM buthionine-sulfoximine (BSO) for 24 h and part of PBS and Cu_{2-x}S-LT@PLGA group exposed to irradiation (1064 nm, 1.5 W cm², 5 min) after removing drug solution and rinsed with PBS. These cells were treated with trypsin and collected by centrifuge, then treated with proper volume of protein removal reagent S. Samples were frozen by liquid nitrogen and thawed at 37 °C for at least three times. After placed at 4 °C for 5 min, the extract was collected by centrifuging at 4 °C at 10000 rpm for 5 min. Proper volume of extract and proper volume detection solution was mixed in 96-well plates and incubated at 25 °C for 30 min. The intracellular GSH was determined by the absorbance at 405 nm using a microplate reader.

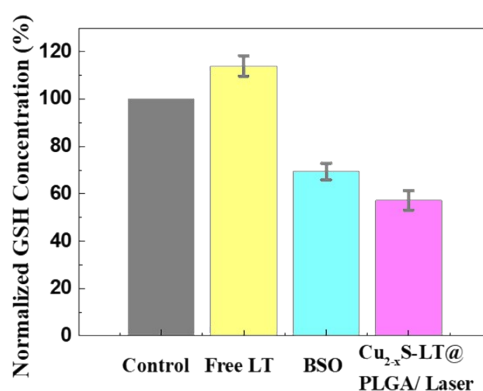


Fig. S2 Intracellular GSH level change with the incubation of LT (4 μ M), BSO (500 μ M), and Cu_{2-x}S-LT@PLGA/ laser (1064 nm, 1.5 W cm², 5 min) against MHCC97H cell.

The test of $\cdot\text{OH}$ generated via TMB

3,3',5,5'-Tetramethylbenzidine dihydrochloride (TMB) color reaction was used to determine the capacity of $\text{Cu}_{2-x}\text{S}@\text{PLGA}$ NPs to produce $\cdot\text{OH}$ in vitro. Add 100 μL of $\text{Cu}_{2-x}\text{S}@\text{PLGA}$ NPs (640 mg mL^{-1}) to the PBS buffer ($\text{pH} = 5.5$), then 50 μL of H_2O_2 solution (500 mM) were add, and finally 100 μL of TMB (5 mM) were added (the total volume is controlled to 2 mL). The absorbance of the color reaction within 2 min was determined by UV-visible spectrophotometry.

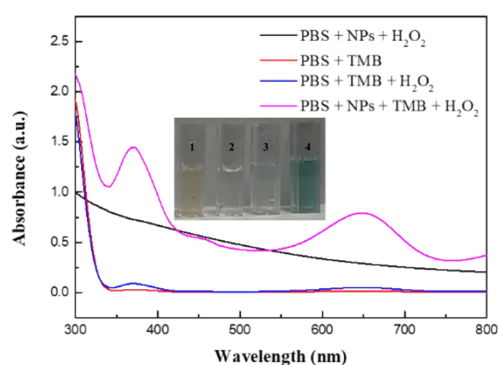


Fig. S3 UV-vis absorption spectra of the catalyzed oxidation of TMB (oxTMB) in an acid environment ($\text{pH} 5.5$).

In vivo blood circulation and tissue distribution test

Mice were injected with 200 μL of $\text{Cu}_{2-x}\text{S-LT@PLGA}$ dispersion (6.4 mg mL^{-1} , 40 mg kg^{-1}) at different time intervals (0 h, 15 min, 30 min, 1 h, 2 h, 4 h, 8 h, 12 h, 24 h and 48 h). Blood samples ($10 \mu\text{L}$) were collected from the tail vein to evaluate the circulation of $\text{Cu}_{2-x}\text{S-LT@PLGA}$ in the blood. The blood samples were then dissolved in aqua regia and shaken all day. Finally, the content of Cu ions in each blood sample was determined by ICP-OES analysis.

For *in vivo* biodistribution determination, tumor-bearing mice were euthanized at 0 h, 12 h, 24 h, and 48 h after $\text{Cu}_{2-x}\text{S-LT@PLGA}$ injection. The main organs, including the heart, spleen, kidney, lung, liver and tumors, were collected, weighed, and then completely dissolved in aqua regia. The concentrations of Cu ions were determined by ICP-OES.

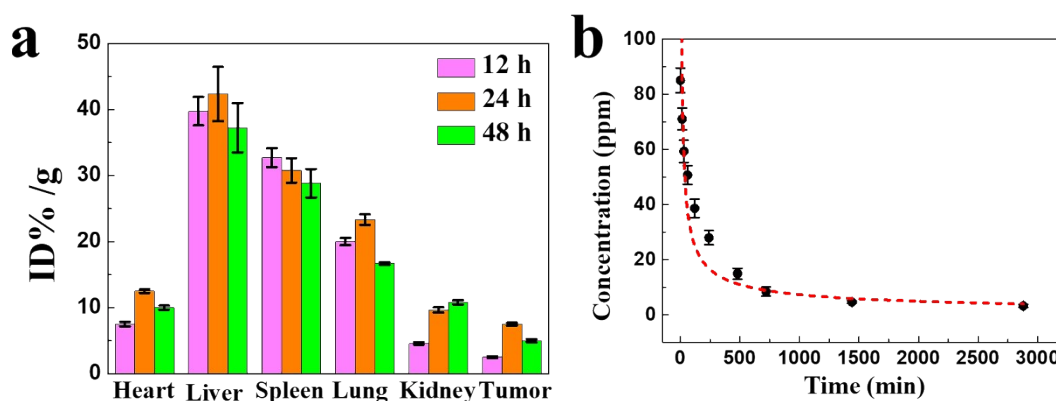


Fig. S4 *In vivo* pharmacokinetics studies. (a) The biodistribution of Cu in the main tissues after the intravenous administration of $\text{Cu}_{2-x}\text{S-LT@PLGA}$ into tumor-bearing mice for 12 h, 24h and 48 h ($n = 3$). (b) The blood-circulation curve of intravenously injected $\text{Cu}_{2-x}\text{S-LT@PLGA}$ ($n = 3$).

Investigation of the vascular inhibitory effect of Cu_{2-x}S-LT@PLGA

The anti-angiogenesis effect was analyzed through immunohistochemistry data of tumor tissues, which were stained by CD-31 (DAB staining solution) /hematoxylin. The male BALB/c-nu mice bearing MHCC97H tumors were treated with Cu_{2-x}S-LT@PLGA NPs, PBS, only laser, free LT, Cu_{2-x}S-LT@PLGA NPs-laser, Cu_{2-x}S@PLGA NPs+laser and Cu_{2-x}S-LT@PLGA NPs +laser. The tumors were excised and fixed with 4% formalin after two weeks, then the excised tumor sections were incubated with CD-31 antibody/hematoxylin and treated with DAB staining solution, covered with a coverslip, and observed using an optical microscope.

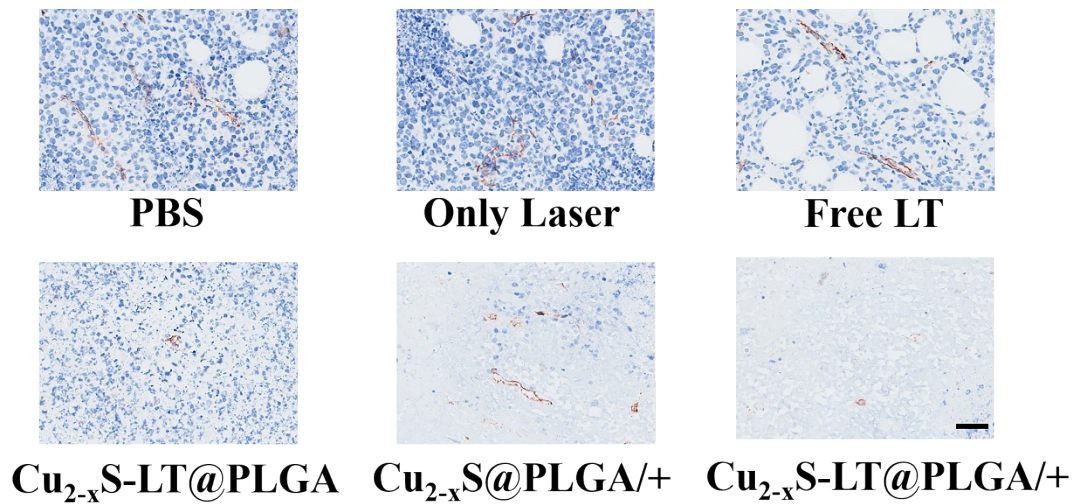


Fig. S5 Immunohistochemistry image of treatments on the MHCC97H xenograft Tumor was investigated by CD-31 staining (DAB staining solution, brown, denoted blood vessels) and hematoxylin staining (blue, denoted cells nuclei). The scale bar is 50 μ m.

References

1. W. Ren, Y. Yan, L. Zeng, Z. Shi, A. Gong, P. Schaaf, D. Wang, J. Zhao, B. Zou, H. Yu, G. Chen, E. M. B. Brown and A. Wu, *Advanced Healthcare Materials*, 2015, **4**, 1526-1536.
2. A. D. Bokare and W. Choi, *Journal of Hazardous Materials*, 2014, **275**, 121-135.
3. J. F. Perez-Benito, *Monatshefte für Chemie / Chemical Monthly*, 2001, **132**, 1477-1492.